

Interionic potentials, pseudopotentials, and the structure factor of liquid lead

M. W. C. Dharma-wardana and G. C. Aers

National Research Council of Canada, Ottawa, Canada K1A 0R6

P. W. M. Jacobs and Z. A. Rycerz

University of Western Ontario, London, Ontario, Canada N6A 3K7

K.-E. Larsson

Royal Institute of Technology, S-11428 Stockholm, Sweden

(Received 11 August 1987)

We study the experimental structure factor of liquid Pb using the modified hypernetted-chain equation. The dependence of the pair potential on the structural environment is related to the electron effective mass which changes discontinuously at the melting point while the pseudopotential remains invariant. A solid-phase pair potential derived from liquid-phase results gives good elastic constants, phonon data, and the low-temperature electronic specific heat, although based only on a local two-parameter pseudopotential.

Recently, there has been much interest in extracting information about interionic potentials and pseudopotentials from liquid-structure data obtained from neutron scattering or x-ray diffraction experiments.¹⁻⁴ High-quality data for the structure factor $S(k)$ are becoming available, often at several temperatures. The variation in temperature introduces a continuous modification of the pair-distribution function $g(r)$ describing the environment around any given ion. Also, in liquid-structure calculations, the effective pair potentials sample all values of position r , and not just the lattice positions appropriate to a crystalline solid. Hence liquid-structure data provide a testing ground for the transferability of pair potentials from one $g(r)$ to another at a different temperature, and then to the environment of the crystalline solid. This is also an indirect test of the assumption of transferability inherent in the approach to the construction of pair potentials where a phenomenological form is fitted to some property or to large-scale total-energy calculations,^{5,6} for a variety of structures or clusters. The problem is also of interest in studies of grain boundaries,⁷ disordered materials, embedding problems,⁸ etc., where the immediate environment⁹ around a given ion is different to that in the homogeneous solid. Other areas of interest are in molecular-dynamics simulation studies,¹⁰ where it would be useful to know how a pair potential should be modified to take account of the environment, and in equation of state studies where a wide range of temperatures and densities have to be spanned in an economical manner.

In this Brief Report we examine recent experimental data for the structure factor of liquid lead at several temperatures. We extract the effective Pb pseudopotential V_{i-e} for the electron-ion interaction and the effective ion-ion pair-potential U_{i-i} using the modified hypernetted-chain (MHNC) fitting method,^{1,11} which has already been

tested in a number of cases. The MHNC equation relates U_{i-i} to $g(r)$ by $g(r) = \exp[-\beta U_{i-i}(r) + N(r) + B(r)]$. The nodal function $N(r)$ can be expressed in terms of $g(r)$, while $B(r)$ is the bridge term.¹² The pair potential and pseudopotential are taken to be related by the form (atomic units)

$$U_{i-i}(k) = Z^2 V_k - |V_{i-e}(k)|^2 \chi(k, m^*), \quad (1)$$

where $V_k = 4\pi/k^2$ and $\chi(k, m^*)$ is the electron-gas response function involving an effective electron mass $m^* = r_s^*/r_s$. The electron sphere radius $r_s = r_0/Z^{1/3}$, with r_0 the Wigner-Seitz radius. For Pb, the ionic charge is $Z = 4$. Expressing k in units of the Fermi momentum $k_F = 1/(ar_s)$, $\alpha = (4/9\pi)^{1/3}$, the electron response function times V_k can be written as

$$V_k \chi(k, m^*) = \frac{4\lambda m^* F(k)}{k^2 + [1 - G(k, r_s^*)] 4\lambda m^* F(k)}, \quad (2)$$

where $\lambda = \alpha r_s / \pi$ and $G(k, r_s^*)$ is the local-field correction. $F(k)$ is the dimensionless Lindhard function given by

$$F(k) = \frac{1}{2} \left[1 + \frac{1}{k} \left[1 - \frac{k^2}{4} \right] \ln \left| \frac{1+k/2}{1-k/2} \right| \right]. \quad (3)$$

Several models of the $G(k, r_s)$ are available. Here we have used the local-density approximation (LDA),¹³ the Geldart-Taylor (GT),¹³ and Ichimani-Utsumi¹³ (IU) models. Note that the local field is evaluated at r_s^* and hence the effective mass of the electron enters into the local field as well. A simple pseudopotential, defined by a well depth A_0 and a cutoff radius R_0 was found to be adequate for the present study, as in the case¹¹ of Ge, which is also a four-valent liquid metal in the same group as lead, and having a filled d shell. Thus,

$$V_{i-e}(k) = \left[\frac{A_0 R_0}{Z} \sin(kR_0) / kR_0 - \left(\frac{A_0 R_0}{Z} + 1 \right) \cos(kR_0) \right] ZV_k. \quad (4)$$

Hence the adjustable parameters of the problem are A_0 , R_0 , and m^* . The latter involves the environment around a given ion as felt by the electrons and should be a structure-sensitive quantity. Its importance in regard to the structure of liquid Ge was established in Ref. 11. The pseudopotential itself is not unique,¹⁴ but the effective pair potential $U_{i-i}(r)$ should be model independent in the sense that we should recover the same $U_{i-i}(r)$ irrespective of the model used for $G(k, r_s^*)$. In this study we have found that the $U_{i-i}(r)$ obtained by MHNC fitting is (within 1%) independent of whether we use the LDA, GT, or the IU form of $G(k, r_s^*)$. Hereafter we shall therefore restrict ourselves to the LDA form of the local field.

This description is valid even if there are three-body terms, d -electron tight-binding effects, etc., in which case the parameters A_0 , R_0 , and m^* will define *effective* potentials. If such effects are preponderant, then the utility or transferability of the parametrization will be severely hampered. This can only be determined by applying the resulting potential to different structural situations, as done in this study.

For a given "trial" choice of the parameters A_0 , R_0 , and m^* we solve the modified hypernetted-chain equation using the Rosenfeld-Ashcroft-Lado¹² hard-sphere model to describe the bridge term. This simple prescription introduces an additional parameter η (hard-sphere packing fraction) which does not enter the pair potential $U_{i-i}(r)$. These parameters are varied to obtain the best fit to the experimental data, viz., $S(k)_{\text{expt}}$, available in some range $k_{\text{min}} < k < k_{\text{max}}$. Note that we do *not* extrapolate the experimental data by attaching tails, nor do we Fourier transform $S(k)_{\text{expt}}$ at any stage of the calculation.

The fit to experimental $S(k)$ data^{15,16} obtained for Pb (melting point, 600 K) at two temperatures, 613 and 1163 K, are shown in Fig. 1. The $S(0)$ values of the fits agree well (see inset) with available compressibility data. The large- k regime (not shown) was also reproduced very well. Equally good fits [to well within the error in $S(k)_{\text{expt}}$, viz., about 2%, except for small k , where experimental errors are larger] were obtained at 643 and 843 K, but are not shown here. Figure 2 shows the pair potentials obtained at these (liquid) temperatures, together with a potential at 300 K referred to later. Figure 2 clearly shows the unraveling of a higher-energy Friedel oscillation in the pair potential at the higher temperature. The density of Pb decreases by about 7% from 613 to 1163 K, leading to a change in Fermi momentum. Ignoring this and the implications of Fig. 2, if we use the 613-K potential to calculate $S(k)$ at 1163 K, results which are visually almost as good as those (but having a significantly larger mean square error) from the 1163-K potential of Fig. 2 are obtained. In this sense, the 613-K potential is approximately transferable in the liquid

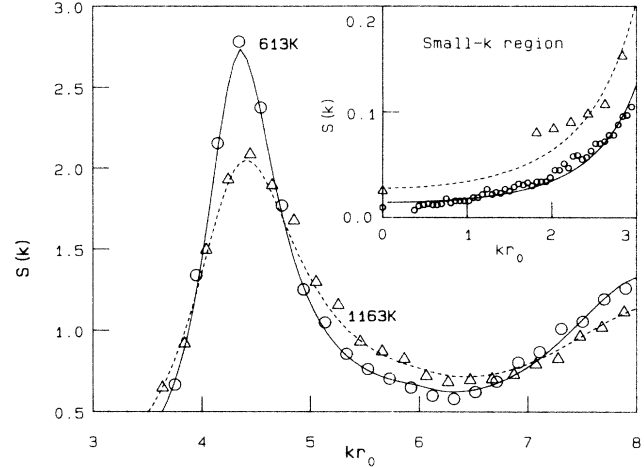


FIG. 1. Comparison of calculated and experimental $S(k)$ at 613 and 1163 K; experimental points are indicated by circles and triangles, respectively. The calculated curves use the pseudopotential of Eq. (4). Inset: small- k region.

phase. However, if the 613-K potential is used to calculate elastic constants and phonons of Pb in the solid phase, imaginary modes are obtained, showing that the pair potential is not transferable to a different environment. However, we have found that the pseudopotential parameters A_0 and R_0 remain constant (to within 2.0%) from 613 and 1163 K, while the effective mass m^* changes progressively, as in Fig. 3. Hence a more theoretically sound approach is to assume that the pseudopotential is transferable, while m^* —which governs the response function—should be chosen appropriately for each responding environment.

We now attempt to transfer the pseudopotential obtained from liquid-structure data to a calculation of the properties of solid Pb. A_0 and R_0 define the well depth

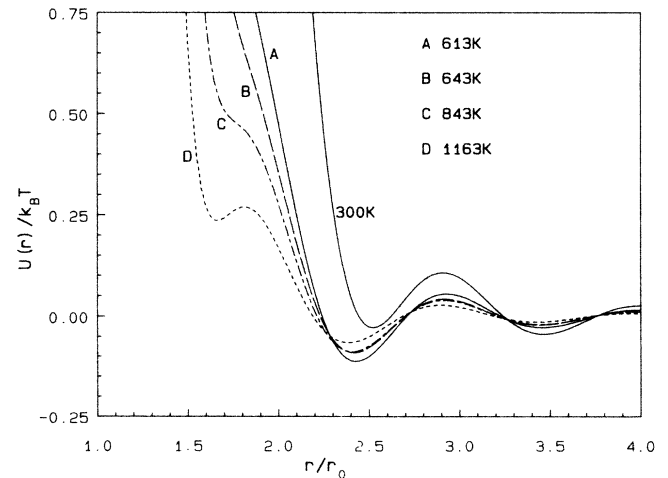


FIG. 2. Ion-ion pair potentials at 613–1163 K are obtained by MHNC fitting to the liquid-structure data (Refs. 15 and 16). The potential at 300 K (solid phase) is derived from the Pb pseudopotential common to the liquid-phase potentials.

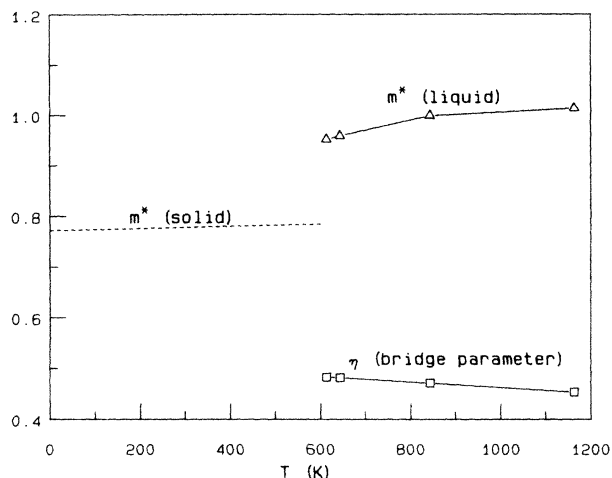


FIG. 3. Variation of the electron effective mass m^* and the hard-sphere packing fraction η used in the MHNC equation (Ref. 12).

and cutoff radius for the Pb ion and hence may be considered a property of the ion rather than that of the environment defined by the responding electron gas. Hence we have retained the A_0 and R_0 values (see Table I) obtained from the liquid-structure fits, but have redetermined m^* to give the best least-squares fit to the elastic constants¹⁷ of Pb at 300 K. The resulting pair potential with $m^*=0.7785$ is shown in Fig. 2. Using elastic constant data at other temperatures, the variation of m^* in the solid phase as a function of temperature can be obtained, as shown in Fig. 3. m^* increases by 0.5% for solid Pb, for the range 0–300 K. In the liquid phase, for the range 613–1163 K, m^* increases by about 5%. Hence, in each phase the pair potential is approximately constant, but more so in the solid. However, if we consider a solid with defects, vacancies, etc., different values of m^* will become locally appropriate.

The value of m^* at 100 K, viz., 0.7737 can be used to calculate the phonon-enhanced effective mass m^* (using the known electron-phonon enhancement factor of 1.55), and hence the coefficient (γ) of the linear (electron) term in the specific heat. We get $\gamma=2.977 \text{ mJ mol}^{-1} \text{ deg}^{-2}$, in agreement with the experimental value ($2.98 \text{ mJ mol}^{-1} \text{ deg}^{-2}$). In Table I we give the experimental and calculated elastic constants at 300 and 100 K. The agreement found at 100 K is typical of calculations at other temperatures. We have also calculated the phonon spectrum at 120 K for the wave vector Q along the [100] direction. Good agreement with experiment¹⁸ at 120 K is obtained for Q values up to 70% of the zone; the Kohn anomalies are suppressed as they should be, but the downward dispersion for larger Q is not properly reproduced. However, given the extreme simplicity of the potential, and the somewhat complicated Fermi surface of Pb, etc., it is not reasonable to expect better agreement at high Q near the zone edge.

In Fig. 4 we show the $g(r)$ obtained by a molecular-

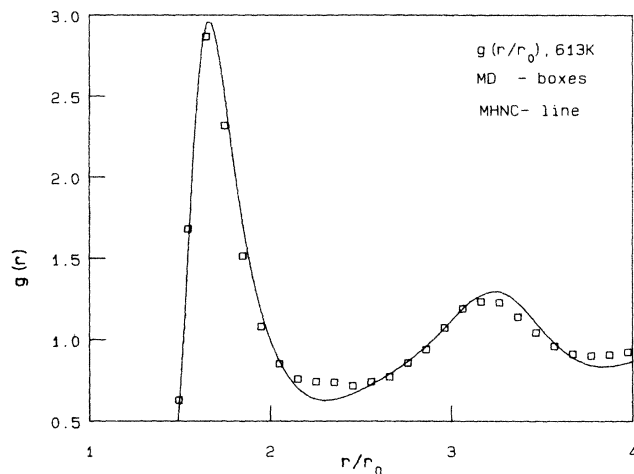


FIG. 4. Comparison of the $g(r)$ at 613 K. Calculated with the MHNC equation and by MD simulation using the potential at 613 K.

dynamics (MD) simulation using the 613-K potential. The $g(r)$ obtained from the MHNC calculation is also given. If the bridge term were exact, and if the MD simulation were exact, the two curves should be identical. The differences suggest that a more careful modeling of the bridge term may be needed. The diffusion coefficient D determined from an analysis of mean-square displacements in the MD simulation ($D=2.83 \times 10^{-5} \text{ cm}^2/\text{s}$) or from the velocity autocorrelation function ($D=2.74 \times 10^{-5} \text{ cm}^2/\text{s}$) may be compared with the experimental value [$(2.2 \pm 0.3) \times 10^{-5} \text{ cm}^2/\text{s}$]. The Einstein frequency from MD simulations and from experiment is 6.2 and $7.6 \pm 0.9 \text{ meV}$, respectively. To obtain better agreement, the pseudopotential may have to include nonlocality effects, etc., while the pair potential may require terms beyond two-body interactions. Details of these more elaborate studies and MD simulations will be published elsewhere.

m^* changes by about 20% from the solid to the liquid. The volume increment and entropy change ($\Delta S/Nk_B$) are 3.5% and 0.96 (cf. sodium, 2.5% and 0.85), respectively. The large change in m^* is probably related to a rearrangement of the Fermi surface upon melting. Small (e.g., 3%) changes in the structure can have large effects

TABLE I. The elastic constants (in 10^{12} dyn/cm^2) of lead at 300 and 100 K calculated from the three-parameter pair potential with $A_0=-1.6869 \text{ a.u.}$, $R_0=1.6707 \text{ a.u.}$, and LDA screening with $m^*=0.7785$. Experimental values are in parentheses. Values at 300 K were used to determine m^* .

T (K)	C_{11}	C_{12}	C_{44}
300	0.483 (0.495)	0.406 (0.423)	0.158 (0.149)
100	0.518 (0.538)	0.432 (0.444)	0.170 (0.180)

on m^* , and, hence, on the effective pair potential.

The discontinuity in m^* seen in Fig. 3 from the liquid to the solid suggests that in modeling rapidly quenched metal solids,¹⁹ etc., the appropriate pair potential may *not* be that of the solid. Probably a potential (or an ensemble of potentials) derived from the m^* of the various stages of quenching may be more appropriate.

In conclusion, we have shown that a simple pseudopo-

tential defined by a well-depth parameter A_0 and a cutoff radius R_0 can be used to describe the properties of solid and liquid lead, if the pair potential includes the variation of the electron effective mass m^* , as a function of the structural environment. The pair potential is not transferable if the structural environment seen by the electrons changes significantly, modifying the value of m^* which scales the response of the electron gas.

¹M. W. C. Dharma-wardana and G. C. Aers, *Phys. Rev. B* **28**, 1701 (1983); *Phys. Rev. Lett.* **56**, 1211 (1986).

²W. Schommers, *Phys. Rev. A* **28**, 3599 (1983); *Phys. Rev. Lett.* **58**, 427 (1987).

³D. Levesque, J. J. Weis, and L. Reatto, *Phys. Rev. Lett.* **54**, 451 (1985).

⁴K. E. Larsson and W. Gudowski, *Phys. Rev. A* **33**, 1968 (1986).

⁵F. H. Stillinger and T. A. Weber, *Phys. Rev. B* **31**, (1985); see also R. Biswas and D. R. Hamann, *Phys. Rev. Lett.* **55**, 2001 (1985).

⁶J. Tersoff, *Phys. Rev. Lett.* **56**, 632 (1986).

⁷See papers in *J. Phys. (Paris) Colloq.* **43**, C6 (1982).

⁸M. S. Daw and M. I. Baskes, *Phys. Rev. Lett.* **50**, 1285 (1983).

⁹A. E. Carlsson, *Phys. Rev. B* **32**, 4866 (1985).

¹⁰R. Taylor, *J. Phys. (Paris) Colloq.* **46**, C4-309 (1985).

¹¹G. C. Aers, M. W. C. Dharma-wardana, M. Gibb, and François Perrot, *Phys. Rev. B* **33**, 4307 (1986), and Ref. 1.

¹²Y. Rosenfeld and N. W. Ashcroft, *Phys. Rev. A* **20**, 1208 (1979); see also F. Lado, S. M. Foiles, and N. W. Ashcroft, *ibid.* **28**, 2374 (1983).

¹³See Ref. 1 for details.

¹⁴V. Heine and D. Weaire, in *Solid State Physics*, edited by H. Ehrenreich, F. Seitz, and D. Turnbull (Academic, New York, 1970), Vol. 24, p. 249.

¹⁵U. Dahlborg, M. Davidovic, and R. E. Larsson, *Phys. Chem. Liq.* **6**, 149 (1977).

¹⁶L. G. Olsson and U. Dahlborg, *Phys. Chem. Liq.* **11**, 225 (1982).

¹⁷D. L. Waldorf and G. A. Alers, *J. Appl. Phys.* **33**, 3266 (1962).

¹⁸B. N. Brockhouse, T. Arase, G. Caplioti, R. R. Rao, and A. D. B. Woods, *Phys. Rev.* **128**, 1099 (1962).

¹⁹*Glassy Metals*, edited by H. Beck and H.-J. Güntherodt (Springer-Verlag, Berlin, 1983).